

# 263F Fall 2023 Homework 1

Yuchen Li and Prof. Khalid\*, MAE Department, UID: 305482394

**Abstract**—This assignment mainly addressed the questions asked in three deliverables from Chapter 4. The plots and figures will be shown and followed by corresponding discussions. We used a discrete method to numerically simulate the motions of connected spheres falling and the deformation of a elastic beam bending.

## I. 4.2: THREE-CONNECTED SPHERES

Considering that three spheres are connected with two linear springs and one torsional spring, the original configuration is horizontal at rest and it starts falling under gravity in a viscous fluid. We construct a Degrees of Freedom (DoF) vector to simulate such a process and all the parameters come from Lecture Notes. The continuous equations of motion is as follows:

$$\mathbf{q} = [x_1, y_1, x_2, y_2, x_3, y_3]^T$$

$$\mathbf{M}\ddot{\mathbf{q}} + \frac{\partial E^{elastic}}{\partial \mathbf{q}} + \mathbf{C}\dot{\mathbf{q}} - \mathbf{W} = \mathbf{0}, \quad (1)$$

where  $\mathbf{M}$  is Mass matrix,  $\frac{\partial E^{elastic}}{\partial \mathbf{q}}$  is Energy gradient,  $\mathbf{C}$  is Damping matrix and  $\mathbf{W}$  is Weight vector. Since the numerical simulation can only deal with discrete time, equation 1 can be further expressed in implicit and explicit ways with  $t_k$  and  $t_{k+1}$ .

### A. Implicit Case

$$\frac{\mathbf{M}}{\Delta t} [\dot{\mathbf{q}}(t_{k+1}) - \dot{\mathbf{q}}(t_k)] + \frac{\partial E^{elastic}}{\partial \mathbf{q}} + \mathbf{C}\dot{\mathbf{q}}(t_{k+1}) - \mathbf{W} = \mathbf{0}$$

$$\dot{\mathbf{q}}(t_{k+1}) = \frac{\mathbf{q}(t_{k+1}) - \mathbf{q}(t_k)}{\Delta t}, \quad (2)$$

where  $\mathbf{q}(t_k)$  and  $\dot{\mathbf{q}}(t_k)$  are known from previous time step.  $\mathbf{q}(t_{k+1})$  is computed by solving equation 2 with Newton's method and then  $\dot{\mathbf{q}}(t_{k+1})$  can be updated accordingly.

### B. Explicit Case

$$\frac{\mathbf{M}}{\Delta t} [\dot{\mathbf{q}}(t_{k+1}) - \dot{\mathbf{q}}(t_k)] + \frac{\partial E^{elastic}}{\partial \mathbf{q}} + \mathbf{C}\dot{\mathbf{q}}(t_k) - \mathbf{W} = \mathbf{0}$$

$$\mathbf{q}(t_{k+1}) = \mathbf{q}(t_k) + \dot{\mathbf{q}}(t_{k+1})\Delta t, \quad (3)$$

where  $\dot{\mathbf{q}}(t_{k+1})$  is calculated directly from equation 3 with data from previous time step and then  $\mathbf{q}(t_{k+1})$  can be updated accordingly.

\*This work was supported by Prof. Khalid's template codes in lecture

### C. Plots and Discussions

Q1: The following figure indicates the shape of the structure at  $t = \{0, 0.01, 0.05, 0.10, 1.0, 10.0\} \text{ sec}$ . The middle sphere falls more compared with the other two since it is heavier, which makes sense in simulation and reality.

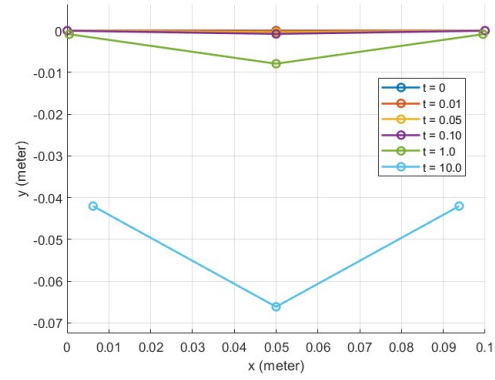


Fig. 1. Shapes of structure evolving

Furthermore, the position (bottom left) and velocity (bottom right) along  $y$ -axis of  $R_2$  is as follows. The velocity has a dramatic fall at the beginning but then converges to some constant value.

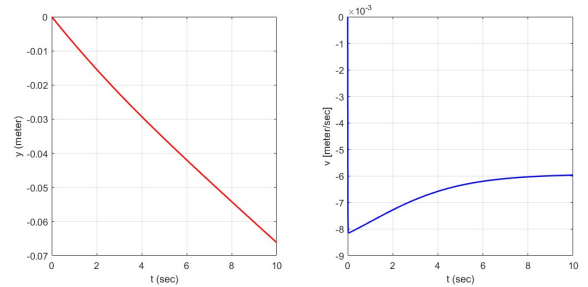


Fig. 2. Falling process of  $R_2$

Q2: As shown in figure 2, the terminal velocity of the system is around  $-6 \times 10^{-3} \text{ m/s}$ . Although there is a tiny deviation between  $R_2$  and  $R_1 \& R_3$  due to the mass difference, they behave similarly.

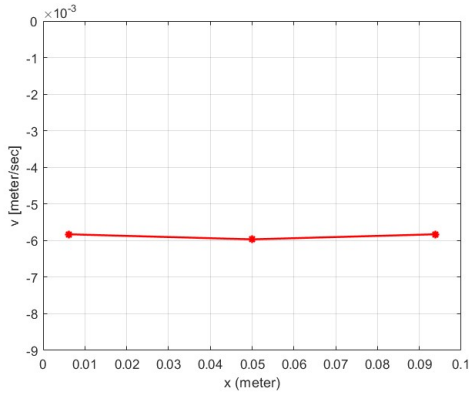


Fig. 3. Terminal velocity of the system

Q3: When all the radii are the same, i.e.  $R_1 = R_2 = R_3$ , we intuitively suppose that the structure would remain horizontal when falling. The simulation gives us the following structure evolving that agrees to our assumption.

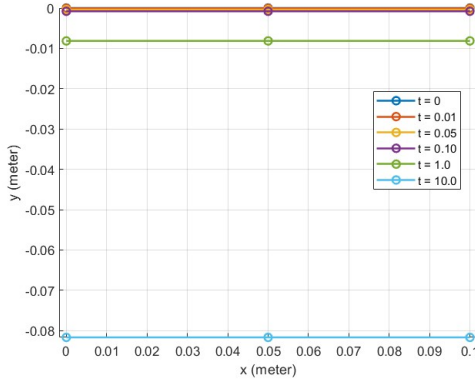


Fig. 4.  $R_1 = R_2 = R_3 = 0.025$

Q4: By changing the time step size ( $\Delta t$ ), we observed that the implicit method is not sensitive to  $\Delta t$  and the algorithm can remain stable with a comparatively big step, i.e.  $\Delta t = 0.1$  s. However, the equation is more complicated than that in the explicit method and needs iterative calculations.

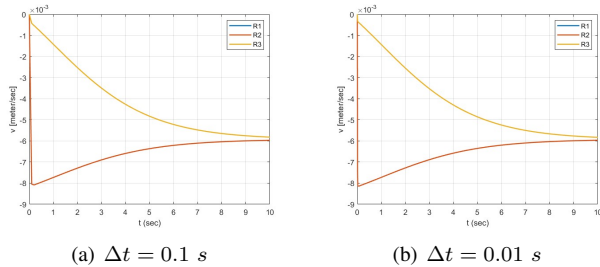


Fig. 5. Velocities of the system (Implicit Method)

In contrast, the explicit method does have simpler equations but requires ( $\Delta t$ ) to be much smaller for the stability of the algorithm, which consumes longer time consequently. In our study, even if  $\Delta t = 10^{-4}$  s, the simulation blows up and diverges to infinity.

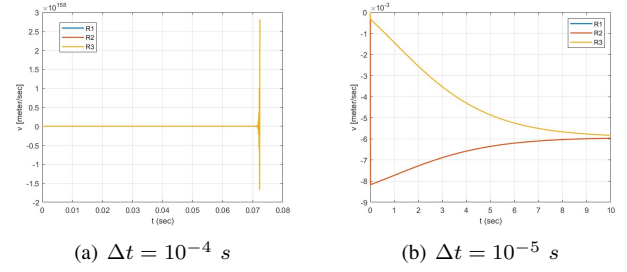


Fig. 6. Velocities of the system (Explicit Method)

#### II. 4.3: N-CONNECTED SPHERES

To generalize the implicit simulator such that the beam is composed of  $N$  nodes ( $N$  is an odd number), the Mass matrix, Damping matrix and Weight vector need to be augmented accordingly. We applied a "for-loop" solver that combines Function and Jacobian calculations to simulate the system. The total time is 50 seconds with the step to be  $\Delta t = 0.01$  s and the number of sphere is  $N = 21$ . Here are the results and related discussions.

Q1: The following plot shows the vertical position and velocity of the middle node with time. It indicates that the terminal velocity is around  $-5.83 \times 10^{-3}$  m/s when  $t$  is larger than 5 s.

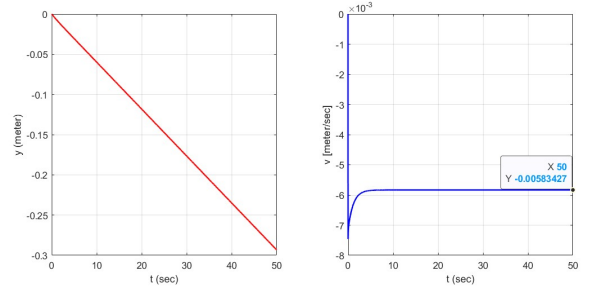


Fig. 7. Falling process of  $R_{11}$

Q2: To record the deformed shape evolving with time, we look at the structure at  $t = \{0, 0.05, 0.10, 1.0, 10.0, 50.0\}$  sec. It is obvious that the shape remains almost the same after  $t = 10.0$  sec, which is a parabolic curve with Node 11 as the vertex.

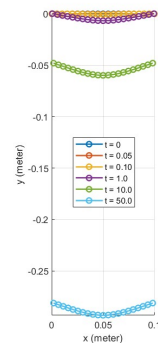


Fig. 8. Shapes of structure evolving

Q3: It is of significance that spatial and temporal discretization are verified for the simulation algorithm. Therefore, we tested their influence independently: When the number of nodes increases, the time step size is set to  $\Delta t = 0.01 \text{ sec}$ ; When the time step size increases, the number of nodes is fixed at  $N = 21$ .

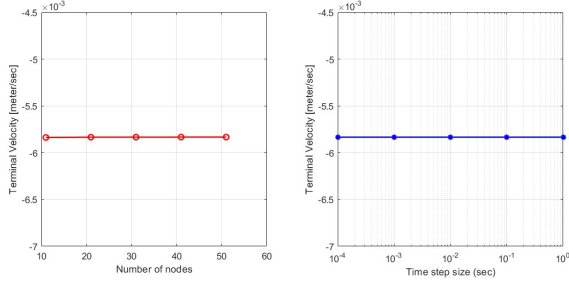


Fig. 9. Terminal velocity vs. the number of nodes (top left) and the time step size (top right)

Figure 9 tells us that the proposed solver is robust in both spatial and temporal discretization. Generally, when the number of nodes increases, the degrees of freedom of the system grow with more stretching and bending energy included. When the time step size increases, the simulation can lose accuracy since the discrete dynamics might blow up when  $\Delta t$  is not sufficiently small even if the continuous system is stable.

### III. 4.4: ELASTIC BEAMS

Similar to the spheres falling, the beam bending can also be simulated using the implicit method. In this section, we look up the solution for a simply-supported aluminum beam subjected to a single point load and compare the simulation results with Euler-Bernoulli beam theory.

The beam can be represented as a mass-spring system with  $dm = \pi(R^2 - r^2)l\rho/(N - 1)$  located at each node with extra boundary conditions introduced: The first node is constrained along both  $x$  and  $y$ -axes and the last node is constrained along  $y$ -axis, i.e.  $x_1(t_{k+1}) = y_1(t_{k+1}) = y_N(t_{k+1}) = 0$ . The viscous force and gravity are replaced with the external force  $P_0$  applied at a node located  $0.75m$  away from the first node. Since there might be no node exactly at  $0.75m$ , we calculate the distance between nodes and point  $P$  to find the closest one and its corresponding index.

```
1 Point = 0.75; % length from the left side
2 [~,ind_P] = min(abs(nodes(:,1) - Point));
3 P0 = 2000;
4 P = zeros(ndof,1);
5 P(2*ind_P) = -P0;
```

Q1: The following plot shows the maximum vertical displacement of the beam as a function of time. The  $y_{max}$  value converges to around  $-0.0370$  at steady state when  $t > 0.05 \text{ s}$ .

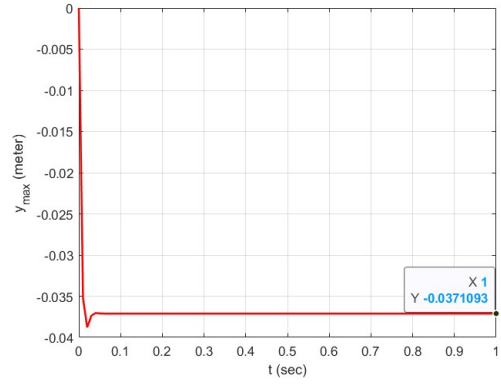


Fig. 10. Maximum vertical displacement of the beam

According to the Euler-Bernoulli beam theory:

$$y_{max} = \frac{Pc(l^2 - c^2)^{1.5}}{9\sqrt{3EI}} \text{ where } c = \min(d, l - d), \quad (4)$$

we work out the theoretical value to be  $y_{max} = -0.0380$ . Comparing the two results, it can be concluded that our simulation is accurate sufficiently.

Q2: The benefit of our simulation is that we can handle both small and large deformations but the Euler-Bernoulli beam theory is only valid in small ones because of nonlinear systems. When the load  $P_0$  increases, the maximum vertical displacements from simulation and theory will diverge gradually. The key point is around  $P_0 = 4000 \text{ N}$  as shown in the figure below.

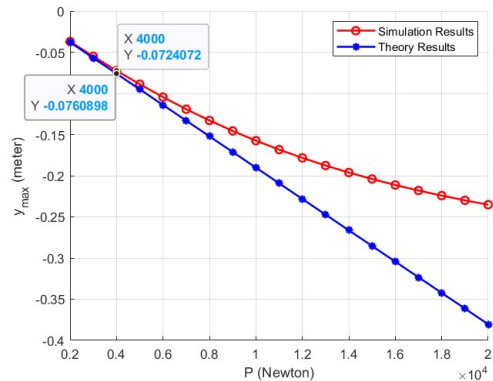


Fig. 11. Simulation and theory difference

## IV. CONCLUSIONS

In this assignment, we applied both implicit and explicit methods to sphere falling simulations and compared the strengths and weaknesses between them. The results indicate that spatial and temporal discretization work well with the algorithm. Considering speed and robustness, the implicit method is preferred and further applied to beam bending simulations. The results agree with the Euler-Bernoulli beam theory but only in small deformations.

## ACKNOWLEDGMENT

This work is based on the code provided by Prof. Khalid in Lecture **263F: *Mechanics of Flexible Structures and Soft Robots*** in Fall 2023. The author modified some parts but still used the functions for calculating gradients, Jacobian and Hessian matrices in the simulation.

## REFERENCES

- [1] M. Khalid Jawed, Sangmin Lim, Discrete Simulation of Slender Structures, pp. 17-23.